The Journal of Veterinary Medical Science

FULL PAPER

Internal Medicine

Changes in gene expression profiles and cytokine secretions in peripheral monocytes by treatment with small extracellular vesicles derived from a canine lymphoma cell line

Akiyoshi TANI[1)], Hirotaka TOMIYASU[1)]*, Hajime ASADA[1,3)], Chen-Si LIN[2)], Yuko GOTO-KOSHINO[1)], Koichi OHNO[1)] and Hajime TSUJIMOTO[1)]

[1)]Department of Veterinary Internal Medicine, Graduate School of Agricultural and Life Sciences, The University of Tokyo, Tokyo, Japan
[2)]Department of Veterinary Medicine, School of Veterinary Medicine, National Taiwan University, Taipei, Taiwan
[3)]Present address: Department of Urology, Northwestern University, Chicago, USA

ABSTRACT. Interactions between tumor and immune cells within the tumor microenvironment play an important role in tumor progression, and small extracellular vesicles (EVs) derived from these tumor cells have been shown to exert immunomodulatory effects on various immune cells, including macrophages and lymphocytes. Although the immunomodulatory effects of small EVs derived from human cancer cells have been intensively investigated, few studies have investigated the effects of lymphoma-derived small EVs on macrophages in both human and veterinary medicine. Here, we evaluated the effects of canine lymphoma-derived small EVs on canine primary monocytes, which are the major source of macrophages in neoplastic tissues. Comprehensive gene expression analysis of these treated monocytes revealed their distinct activation via the Toll-like receptor (TLR) and NF-κβ signaling pathways. In addition, treatment with lymphoma small EVs increased the secretion of MCP-1, which induces the infiltration and migration of monocytes and lymphocytes in neoplastic and cancer tissues. The results of this study indicate that canine lymphoma small EVs activate monocytes, possibly through the activation of TLR and NF-κβ signaling pathways, and induce monocytes to secrete of MCP-1, which might contribute to immune cell infiltration within the tumor microenvironment.

KEYWORDS: diffuse large B-cell lymphoma, dog, monocyte chemotactic protein-1, nuclear factor-kappa β signaling, toll-like receptor signaling

J. Vet. Med. Sci.
84(5): 712–719, 2022
doi: 10.1292/jvms.21-0506

Received: 16 September 2021
Accepted: 22 March 2022
Advanced Epub:
6 April 2022

The tumor microenvironment (TME) plays an important role in the initiation and progression of various tumors [28, 29]. TME is composed of stromal cells, fibroblasts, endothelial cells, and innate and adaptive immune cells. Innate immune cells in the TME include monocytes/macrophages, dendritic cells, neutrophils, myeloid-derived suppressor cells, natural killer cells, and innate lymphoid cells, all of which may initiate immune responses that guide tumor progression [13]. The role of TME in the pathophysiology of human lymphomas is well characterized [24]. In diffuse large B cell lymphoma (DLBCL), which is the most common subtype of human B-cell lymphomas, the number of infiltrative T lymphocytes and macrophages has been reported to be associated with the prognosis of patients [19, 24]. These observations indicate that the interactions between tumor and immune cells are important in the pathophysiology of lymphoma.

Intercellular communication is mediated by membrane proteins, cytokines, hormones, and extracellular vesicles (EVs). Small EVs are defined as EVs less than 200 nm in diameter and released from various cell type which may carry RNA, DNA, or proteins [9, 26]. Small EVs transmit signals to target cells via ligand-receptor interactions, phagocytosis, and endocytosis [9]. Small EVs derived from tumor cells have been shown to modify the functions of immune cells to promote tumor progression via the delivery of various biological components [30]. There have been a few reports describing the roles of small EVs in human DLBCL. These include reports describing their interaction with macrophages to induce tumor-promoting effects within TME [17]. A previous study revealed that small EVs derived from human DLBCL cell lines could be incorporated into THP-1 cells, a human

*Correspondence to: Tomiyasu, H.: atomi@g.ecc.u-tokyo.ac.jp, Department of Veterinary Internal Medicine, Graduate School of Agricultural and Life Sciences, The University of Tokyo, 1-1-1 Yayoi, Bunkyo-ku, Tokyo 113-8657, Japan
(Supplementary material: refer to PMC https://www.ncbi.nlm.nih.gov/pmc/journals/2350/)

acute monocytic leukemia cell line, activating NF-κβ signaling in these cells [31]. However, there have been no studies, to date, investigating the effects of lymphoma-derived small EVs on primary monocytes from the peripheral blood, which are the main source of macrophages within neoplastic tissues.

In addition, in veterinary medicine, there are very few studies discussing the effects of small EVs on neoplastic tissues. Recently, small EVs derived from pro-inflammatory canine macrophages were reported to exhibit apoptotic effects on canine cancer cell lines [15]. Meanwhile, the effects of cancer cell-derived small EVs on immune cells have not been investigated in veterinary medicine.

We previously analyzed the microRNA and protein profiles of canine lymphoma and leukemia-derived small EVs, which were defined in terms of their size and specific protein markers [1]. However, the biological functions of these small EVs remain unclear. Given this, we designed this study to evaluate the immunomodulatory effects of canine lymphoma-derived small EVs on canine primary monocytes and we evaluated the changes in gene expression profile and cytokine secretion in canine primary monocytes treated with canine DLBCL-derived small EVs.

MATERIALS AND METHODS

Cell line validation and culture conditions

We used a canine B-cell lymphoma cell line, CLBL-1, established and validated in a previous study [22] for our experiments. Mycoplasma contamination was excluded using a Takara PCR Mycoplasma Detection Set (Takara Bio Inc., Kusatsu, Japan). The cell line was cultured in RPMI-1640 medium at 37°C, with 10% fetal bovine serum (Biowest, Nuaille, France) and penicillin-streptomycin (Thermo Fisher Scientific, Waltham, MA, USA) in a humidified atmosphere containing 5% CO_2.

Small EV isolation from the culture supernatant of CLBL-1

Small EVs were isolated from the culture medium of CLBL-1 as previously reported [1]. Briefly, 3×10^7 CLBL-1 cells were cultured in growth medium without fetal bovine serum for 24 hr, and small EVs were isolated from cell culture media using a Total Exosome Isolation (from cell culture media) kit (Thermo Fisher Scientific). In the small EV isolation procedure, the culture supernatant was removed after the last centrifugation step, which precipitates the small EVs, according to the manufacturer's instructions. We previously demonstrated that the average size of these small EVs was 100–150 nm and was concordant with the size definition [1, 26]. Isolated small EVs were resuspended in phosphate-buffered saline (PBS) and lysed by RIPA buffer followed by 10 times dilution with distilled water as previously described [25]. The concentration of the obtained protein was measured using a Micro BCA Protein Assay (Thermo Fisher Scientific) following the manufacturer's instructions.

Isolation of primary monocytes

Peripheral blood was collected from healthy beagle dogs kept for experimental purposes in our laboratory, and peripheral blood mononuclear cells (PBMCs) were isolated via gradient centrifugation with Ficoll-Paque (1.077 g/ml; GE Healthcare, Chicago, IL, USA). $CD14^+$ monocytes were isolated from freshly prepared PBMCs using the MACS system (Miltenyi Biotec, Bergisch Gladbach, Germany) with a selection column as previously described, with some modifications [6]. Briefly, PBMCs were incubated with the anti-CD14 mouse monoclonal antibody, TUK4 (Thermo Fisher Scientific), and secondary goat anti-mouse microbeads (Miltenyi Biotec). Thereafter, the incubated cells were positively selected using a selection column (MACS column MS, Miltenyi Biotec) and then washed. This method isolated $CD14^+$ monocytes with a purity of more than 95%, as determined via flow cytometry (Supplementary Fig. 1). This animal experiment was approved by the Animal Care Committee of The University of Tokyo (approval no. P19-120).

Small EV treatments for canine monocytes

Isolated monocytes were seeded in 24-well plates at a concentration of 2×10^5 cells/ml with or without small EVs. The monocytes were cultured in RPMI-1640 medium at 37°C, with 10% exosome-depleted fetal bovine serum (Thermo Fisher Scientific) and penicillin-streptomycin in a humidified atmosphere containing 5% CO_2. Small EVs were added to the monocytes at a final concentration of 80 µg/ml based on the previous reports [2, 3], and the same volume of PBS without small EVs was added to the control groups. After 4 hr of incubation, non-attached cells were discarded [5], and total RNA was extracted from the attached cells using an RNeasy mini kit (Qiagen, Milan, Italy).

RNA sequencing

RNA integrity was assessed using a BioAnalyzer 2100 (Agilent Technologies, Palo Alto, CA, USA), and samples with an RNA integrity number (RIN) of >7.5 were used for RNA-seq. RNA was extracted from monocytes isolated from a healthy dog to minimize variance in gene expression levels between different donors. One microgram of total RNA was amplified using the SMARTer Ultra Low RNA Kit for sequencing (Clontech Laboratories, Mountain View, CA, USA) following the manufacturer's instructions. Next, 0.2 ng of cDNA was subjected to 11 cycles of PCR. The quality of the sequencing library was assessed using a BioAnalyzer 2100, and three cDNA libraries from small EV-treated monocytes and three cDNA libraries from control monocytes were constructed. These libraries were sequenced on the Illumina NovaSeq 6000 platform using a 150-base pair paired-end strategy. Base calling was performed using the Real Time Analysis software (v3.4.4, Illumina, San Diego, CA, USA) and data were demultiplexed and converted to the FASTQ format using bcl2fastq2 software (v2.20, Illumina). Mapping of the reads was conducted using STAR (2.6.0c) and the gene expression levels were calculated and annotated using Genedata Profiler Genome

software (v13.0.11, Genedata Offices, Basel, Switzerland). The genome and gene sequences of *Canis lupus familiaris* (http://www.ncbi.nlm.nih.gov/genome/85?genome_assembly_id=22812) were used for annotation. This sequence data were obtained on October 26, 2019, from ftp://ftp.ncbi.nlm.nih.gov/genomes/all/GCF/000/002/285/GCF_000002285.3_CanFam3.1/. The datasets used and analyzed in the present study are available at the DDBJ Sequenced Read Archive repository with accession number DRA010452.

After filtering the data for genes with low counts across samples (<5 in the sum of six samples), gene count data for each sample were imported into R (version 3.6.3). Tagwise dispersion was calculated and TMM normalization [20] was used to adjust for abundance differences across samples, and differential gene expression analysis was conducted using the EdgeR package and uniquely mapped reads [21]. Hierarchical clustering methods were used to generate dendrograms based on the normalized gene expression data in the genefilter package. DAVID v6.8 (https://david.ncifcrf.gov) was used to investigate the enrichment of Gene Ontology (GO) and Kyoto Encyclopedia of Genes and Genomes (KEGG) pathways for the differentially expressed genes (DEGs). Enriched canonical pathways and upstream regulators of these DEGs were also investigated using Ingenuity Pathway Analysis (IPA, Qiagen).

Reverse transcriptase quantitative PCR (RT-qPCR)

RT-qPCR was performed using monocytes isolated from three different dogs to allow for biological variation. RNA was reverse transcribed using ReverTra Ace qPCR RT Master Mix (TOYOBO, Osaka, Japan) according to the manufacturer's instructions. qPCR was performed using TB Green Premix Ex Taq (Takara) and a Thermal Cycler Dice Real Time System (Takara). *Ornithine decarboxylase antizyme* (*OAZ1*) was used as the reference gene as described previously [12] and the mRNA expression levels of the target genes were normalized against *OAZ1*. The primers used in this analysis are listed in Supplementary Table 1.

Cytokine array analysis

Monocytes were isolated from three different dogs to allow for biological variation, and 2×10^5 cells/ml were then cultured with or without small EVs for 24 hr, and the culture supernatant was collected. RPMI-1640 medium with 10% exosome-depleted fetal bovine serum and penicillin-streptomycin was used as a negative control. The cytokine concentrations in each of these supernatants were quantified using Quantibody Canine Cytokine Array Q1 (RayBiotech, Norcross, GA, USA). These experiments were conducted according to the manufacturer's instructions, and the slides were scanned using an Innoscan 710 microarray scanner (Innopsys, Carbonne, France). Images were then analyzed using GenePixVR Pro 6 Acquisition & Analysis software, and the concentration of each cytokine was calculated using a standard curve prepared using a serially diluted cytokine cocktail. The concentration of each cytokine in the control or small EV-treated monocytes was subtracted from that of the negative control, and these concentrations were compared.

Statistical analysis

In the differential expression analysis using EdgeR, a false discovery rate of less than 0.1 was considered statistically significant. The mRNA and cytokine evaluations were compared using student's *t*-test which were completed using R (version 3.6.3), and *P*-values of less than 0.05 were considered statistically significant.

RESULTS

Identifying DEGs in small EV-treated monocytes

The RNA-seq analysis generated at least 61 million raw reads and had a mapping ratio of >86% for each sample (Supplementary Table 2). Differential expression analysis of the small EV-treated and control monocytes identified 446 DEGs, which were defied as genes with $\log_2$ fold change >|1| and false discovery rate <0.1 (Supplementary Table 3). Of these, 320 were upregulated and 126 were downregulated in response to small EV treatment (Fig. 1A). When we evaluated the annotated genes, we saw that the top three downregulated genes included *integrin beta 5* (*ITGB5*), *eosinophil peroxidase* (*EPX*), and *rap guanine nucleotide exchange factor 4* (*RAPGEF4*), whereas the top three upregulated genes included *Ets homologous factor* (*EHF*), *transmembrane serine protease 6* (*TMPRSS6*), and *C-C motif chemokine ligand 13* (*CCL13*). Hierarchical clustering analysis using these DEGs showed that small EV-treated and control monocytes clustered separately (Fig. 1B).

Validation of the RNA-seq results using RT-qPCR

We went on to evaluate the expression levels of six DEGs, *Interleukin* (*IL)-1β*, *IL6*, *tumor necrosis factor α* (*TNFα*), *ITGB5*, *C-X-C motif chemokine ligand 12* (*CXCL12*), and *OTU deubiquitinase 1* (*OTUD1*) in small EV-treated and control monocytes using RT-qPCR to validate the RNA-seq results. *IL-1β*, *IL6*, and *TNFα* were selected from the upregulated DEGs in small EV-treated monocytes in RNA-seq according to the results of a previous report [4], and other 3 genes were randomly selected from downregulated DEGs in small EV-treated monocytes in RNA-seq. The results demonstrated that the transcription of *IL-1β*, *IL6*, and *TNFα* were significantly upregulated in small EV-treated monocytes when compared to the control, whereas *ITGB5*, *CXCL12*, *and OTUD1* transcription was significantly downregulated in the small EV-treated monocytes compared to the control ($P<0.05$) (Fig. 2), confirming the RNA-seq results.

GO terms, KEGG pathway enrichment, and IPA for DEGs

GO biological processes, GO cellular component, and GO molecular function analysis using extracted DEGs showed that 30, 7, and 13 terms were significantly enriched, respectively (-log10 (*P*)>1.3) (Fig. 3A–C). Among the GO biological process terms,

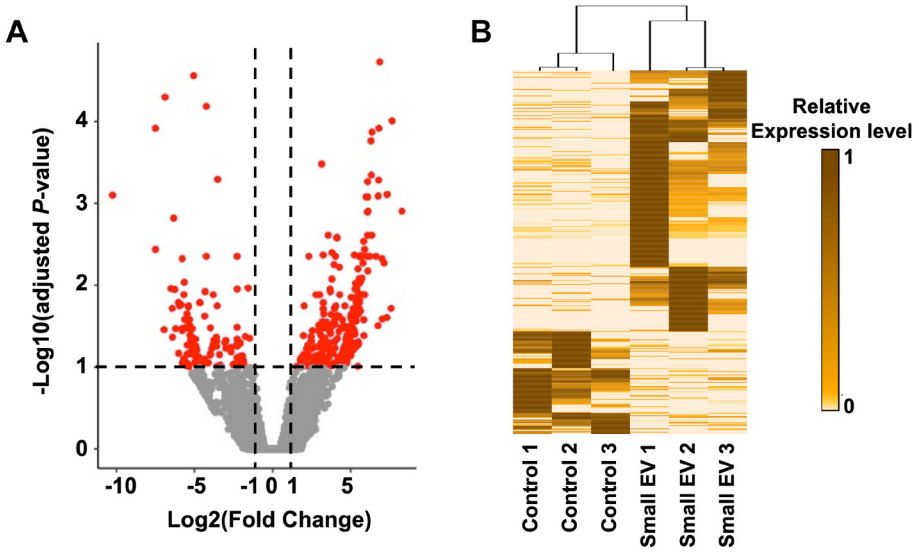

Fig. 1. Extractions of differentially expressed genes (DEGs) and comparisons of gene expression profiles between small extracellular vesicle (EV)-treated and control monocytes. (**A**) Volcano plot showing DEGs in small EV-treated monocytes compared with control monocytes. Red dots indicate DEGs. (**B**) Hierarchical clustering using DEGs in small EV-treated monocytes.

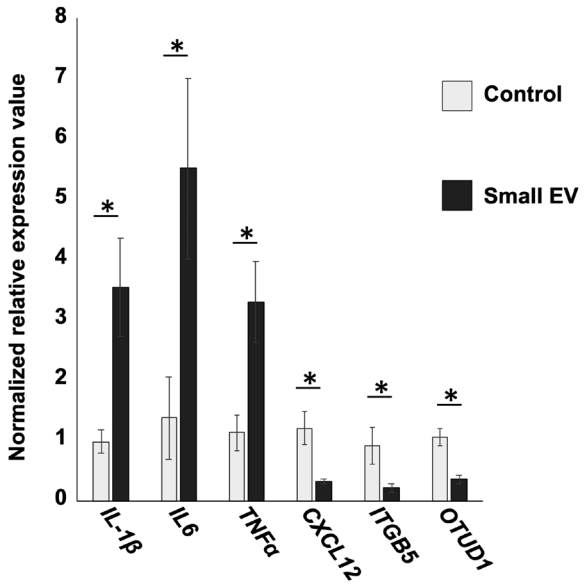

Fig. 2. Comparisons of the expression levels of differentially expressed genes in small extracellular vesicle (EV)-treated and control monocytes using RT-qPCR. Significant differences in relative expression levels were observed in upregulated genes; *Interleukin* (*IL*)*-1β*, *IL6,* and *Tumor necrosis factor* (*TNF*) *α*, and downregulated genes; *Integrin beta 5* (*ITGB5*), *C-X-C motif chemokine ligand 12* (*CXCL12*), and *OTU deubiquitinase 1* (*OTUD1*). N=3 for all tests. * indicates $P<0.05$. Data are shown as the mean ± SD.

immune response and inflammatory response were the most significantly enriched, whereas in the GO cellular component terms, the extracellular space was the most significantly enriched. Cytokine activity was the most significantly enriched in the GO molecular function terms. DAVID-mediated KEGG pathway analysis identified 20 significantly enriched pathways (-log10 (P)>1.3) including the TNF, Jak-STAT, and NF-κβ signaling pathways (Fig. 3D).

Canonical pathway analysis via IPA revealed 14 significantly activated and 2 significantly inhibited pathways, with $P<0.05$ and z-score >|2| (Fig. 4). Significantly activated pathways included the toll-like receptor (TLR) and IL-6 signaling pathways, whereas the significantly inhibited pathways were identified as liver X receptor/retinoid X receptor (LXR/RXR) activation and peroxisome proliferator-activated receptor signaling. Upstream regulator analysis via IPA identified 242 significantly induced and 124 significantly inhibited regulators with $P<0.05$ and z-score >|2| (Supplementary Table 4). The top 10 most significantly induced and inhibited regulators, except for the chemical pathways, are shown in Table 1. The significantly upregulated upstream regulators included TLR4, TLR2, TLR9, TLR3, and NF-κβ.

Quantification of cytokine concentrations via cytokine array analysis

The concentrations of 10 cytokines, IL-2, IL-6, IL-8, IL-10, GM-CSF, MCP-1 (CCL2), RAGE, SCF, TNF-α, and VEGF-A, in the culture supernatant of control and small EV-treated monocytes were evaluated using a cytokine array. Representative figures for each group are shown in Supplementary Fig. 2. Of the 10 cytokines evaluated in this study, only MCP-1 demonstrated significant difference between the two groups, with the average concentration of MCP-1 increasing in the culture supernatant of small EV-treated monocytes (4,021 ± 527 pg/ml) when compared to the control (1,304 ± 894 pg/ml) ($P=0.021$, Fig. 5). When we examined the expressions of *MCP-1* mRNA by RT-qPCR, it was shown that the expression levels of *MCP-1* mRNA expression were significantly higher in small EV-treated monocytes than control ones ($P=0.031$, Supplementary Fig. 3).

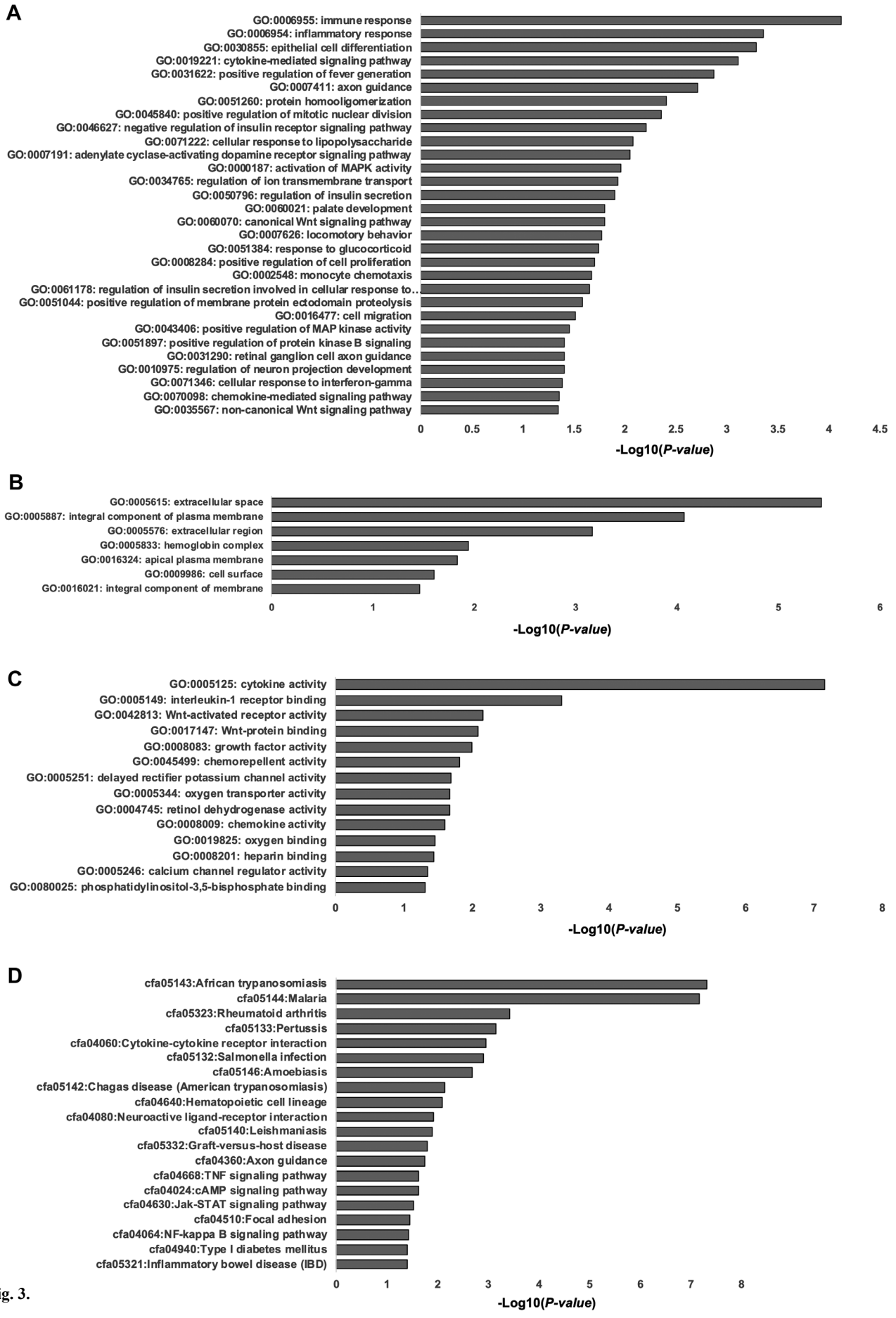
A
GO:0006955: immune response
GO:0006954: inflammatory response
GO:0030855: epithelial cell differentiation
GO:0019221: cytokine-mediated signaling pathway
GO:0031622: positive regulation of fever generation
GO:0007411: axon guidance
GO:0051260: protein homooligomerization
GO:0045840: positive regulation of mitotic nuclear division
GO:0046627: negative regulation of insulin receptor signaling pathway
GO:0071222: cellular response to lipopolysaccharide
GO:0007191: adenylate cyclase-activating dopamine receptor signaling pathway
GO:0000187: activation of MAPK activity
GO:0034765: regulation of ion transmembrane transport
GO:0050796: regulation of insulin secretion
GO:0060021: palate development
GO:0060070: canonical Wnt signaling pathway
GO:0007626: locomotory behavior
GO:0051384: response to glucocorticoid
GO:0008284: positive regulation of cell proliferation
GO:0002548: monocyte chemotaxis
GO:0061178: regulation of insulin secretion involved in cellular response to...
GO:0051044: positive regulation of membrane protein ectodomain proteolysis
GO:0016477: cell migration
GO:0043406: positive regulation of MAP kinase activity
GO:0051897: positive regulation of protein kinase B signaling
GO:0031290: retinal ganglion cell axon guidance
GO:0010975: regulation of neuron projection development
GO:0071346: cellular response to interferon-gamma
GO:0070098: chemokine-mediated signaling pathway
GO:0035567: non-canonical Wnt signaling pathway
0 0.5 1 1.5 2 2.5 3 3.5 4 4.5
-Log10(*P-value*)
B
GO:0005615: extracellular space
GO:0005887: integral component of plasma membrane
GO:0005576: extracellular region
GO:0005833: hemoglobin complex
GO:0016324: apical plasma membrane
GO:0009986: cell surface
GO:0016021: integral component of membrane
0 1 2 3 4 5 6
-Log10(*P-value*)
C
GO:0005125: cytokine activity
GO:0005149: interleukin-1 receptor binding
GO:0042813: Wnt-activated receptor activity
GO:0017147: Wnt-protein binding
GO:0008083: growth factor activity
GO:0045499: chemorepellent activity
GO:0005251: delayed rectifier potassium channel activity
GO:0005344: oxygen transporter activity
GO:0004745: retinol dehydrogenase activity
GO:0008009: chemokine activity
GO:0019825: oxygen binding
GO:0008201: heparin binding
GO:0005246: calcium channel regulator activity
GO:0080025: phosphatidylinositol-3,5-bisphosphate binding
0 1 2 3 4 5 6 7 8
-Log10(*P-value*)
D
cfa05143:African trypanosomiasis
cfa05144:Malaria
cfa05323:Rheumatoid arthritis
cfa05133:Pertussis
cfa04060:Cytokine-cytokine receptor interaction
cfa05132:Salmonella infection
cfa05146:Amoebiasis
cfa05142:Chagas disease (American trypanosomiasis)
cfa04640:Hematopoietic cell lineage
cfa04080:Neuroactive ligand-receptor interaction
cfa05140:Leishmaniasis
cfa05332:Graft-versus-host disease
cfa04360:Axon guidance
cfa04668:TNF signaling pathway
cfa04024:cAMP signaling pathway
cfa04630:Jak-STAT signaling pathway
cfa04510:Focal adhesion
cfa04064:NF-kappa B signaling pathway
cfa04940:Type I diabetes mellitus
cfa05321:Inflammatory bowel disease (IBD)
0 1 2 3 4 5 6 7 8
-Log10(*P-value*)

Fig. 3.

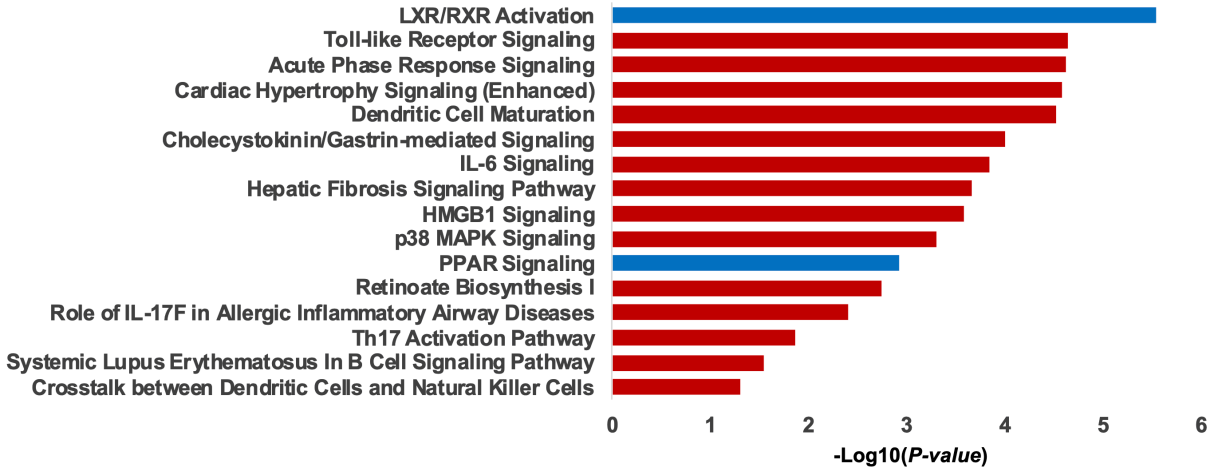

Fig. 4. Histogram showing the enriched pathways in the canonical pathway analysis by Ingenuity Pathway Analysis (IPA) and the differentially expressed genes in small extracellular vesicle (EV)-treated monocytes. Red bar indicates a z-score of >2. Blue bar indicates a z-score of <−2.

Table 1. Top 10 activated and inhibited upstream regulator in small extracellular vesicle-treated monocytes compared with control monocytes

Activated signaling			Inhibited signaling		
Upstream Regulator	Activation z-score	*P*-value of overlap	Upstream Regulator	Activation z-score	*P*-value of overlap
IL1B	4.144	1.34E-08	NR1H2	−2.58	0.000246
EGF	4.142	0.00283	IL37	−2.593	6.75E-08
TLR4	3.798	0.00000134	COL18A1	−2.621	0.000554
JUN	3.619	0.000141	HBB	−2.63	0.000000343
TLR2	3.516	0.0000128	CISH	−2.63	0.000149
TLR9	3.513	0.00000211	HMOX1	−2.73	0.000997
TLR3	3.505	0.00000554	RPSA	−2.771	1.66E-08
NFkB	3.488	0.000731	ZFP36	−2.798	0.000104
F2	3.373	0.00135	miR-155-5p	−2.935	0.00136
IL2	3.349	0.0138	Nr1h	−3.326	0.00000705

DISCUSSION

This study was designed to examine the effects of canine DLBCL cell line-derived small EVs on canine primary monocytes. Our results indicated that treatment with small EVs upregulated the expression of various immune response genes including *IL6* and *TNFα* and activated several intracellular signaling pathways including TLR and NF-κβ signaling in primary monocytes. In addition, small EV-treated monocytes secreted significantly higher concentrations of MCP-1 compared to control monocytes.

Gene ontology and pathway analysis revealed that small EV treatment modulated various pathways, especially those related to inflammatory responses in primary monocytes. Among the modulated pathways, NF-κβ signaling pathway was the most significantly activated in small EV-treated monocytes. These results are consistent with those of a previous study that reported the activation of NF-κβ signaling pathway in THP-1 cells following their treatment with small EVs derived from human DLBCL cell lines [31]. NF-κβ is an important transcription factor that regulates macrophage activation in response to diverse factors [14], thus its activation under these conditions suggest that small EV treatment might activate canine monocytes through this signaling pathway.

Fig. 3. Histograms showing results of gene ontology analyses and pathway analysis using differentially expressed genes extracted from the comparisons of small extracellular vesicle (EV)-treated and control monocytes. (**A**) Histogram showing the enriched gene ontology biological process terms using differentially expressed genes in small EV-treated monocytes. (**B**) Histogram showing the enriched gene ontology cellular component terms using differentially expressed genes in small EV-treated monocytes. (**C**) Histogram showing the enriched gene ontology molecular function terms using differentially expressed genes in small EV-treated monocytes. (**D**) Histogram showing enriched pathways identified by KEGG pathway enrichment analysis of the differentially expressed genes in small EV-treated monocytes.

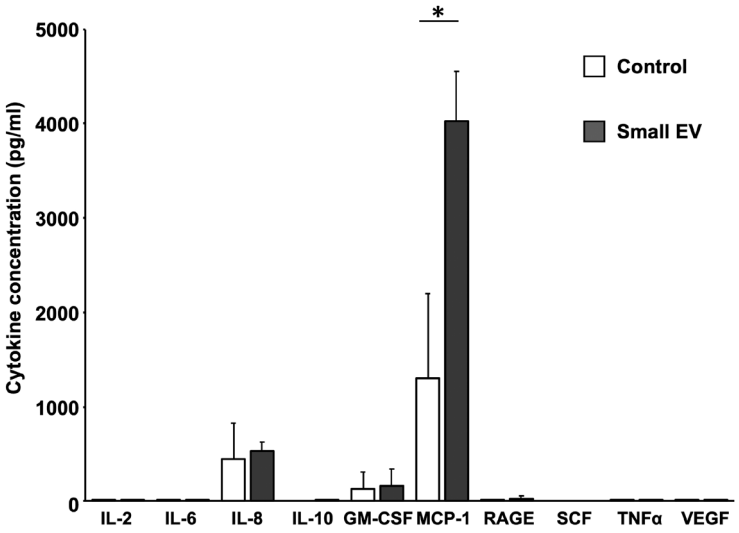

Fig. 5. Comparisons of the concentrations of 10 cytokines in the culture supernatant of control and small extracellular vesicle (EV)-treated monocytes. N=3 for all tests. * indicates $P<0.05$. Data are shown as the mean + SD.

Canonical pathway analysis indicated that TLR signaling was significantly upregulated, and TLR4, TLR2, TLR9, TLR3, TLR5, TLR6, and TLR1 were implicated as upstream regulators. TLRs form part of the pattern recognition receptors and are reported to be activated by various endogenous molecules as well as microbial agonists [23, 27]. It was previously reported that small EVs derived from human tumor cells activate monocytes and macrophages via TLRs. In human ovarian and breast cancer, inhibition of TLRs was reported to repress the secretion of pro-inflammatory cytokines in small EV-treated macrophages [4, 8]. These results imply that there is an interaction between small EVs and TLRs and that this interaction might be important in the activation of these immune cells.

Since TLR activation induces the activation of NF-κβ signaling [7], it is possible that small EVs activate TLR signaling via ligand-receptor interactions and this signaling activates NF-κβ signaling. It is also possible that the components of the small EVs might be released within the monocytes following endocytosis or phagocytosis, and TLR and NF-κβ signaling are activated through this mechanism. We previously revealed that canine DLBCL small EVs included NF-κβ subunit 1, NF-κβ subunit 2, CD40, albumin, complement C3, high mobility group box 1, and c-Rel [1], and these proteins might activate NF-κβ signaling when released within the monocyte cells.

In this study, we noted that the concentrations of MCP-1 were significantly higher in the culture supernatant of small EV-treated monocytes than those of control ones. We also found that the expression of *MCP-1* mRNA was not detected in CLBL-1 cells using RT-qPCR analysis (data not shown) and that MCP-1 protein was not detected within small EVs derived from CLBL-1 in our previous study [1]. In addition, the expression of *MCP-1* mRNA was significantly higher in small-EV treated monocytes compared with control ones. These results suggested that small EVs stimulated monocytes and induced the secretion of MCP-1 from these cells. MCP-1 is produced by many types of cells, including monocytes, and regulates the migration and infiltration of monocytes and lymphocytes [10]. As the expression of MCP-1 is regulated by NF-κβ signaling [18], the results of RNA-seq and cytokine array analysis suggested that the secretion of MCP-1 by monocytes might be induced by the activation of this signaling pathway following small EV treatment. It has been reported that MCP-1 secreted from human tumor or stromal cells recruits monocytes and polarized monocytes to tumor-associated macrophages (TAMs) [11], and TAMs have also been reported to be negative prognostic factors in human DLBCL [16]. Therefore, it is reasonable to speculate that the secretion of MCP-1 from small EV activated monocytes might induce migration and infiltration of these cells into canine DLBCL tissues, and that these monocytes might be associated with the pathophysiology of canine DLBCL.

Unfortunately, we could not show the activation of TLR or NF-κβ signaling using immunofluorescence or immunoblotting analyses. These analyses should be conducted to elucidate the detailed mechanisms of MCP-1 secretion in small EV-treated canine monocytes. In addition, it should be noted that we used only one canine DLBCL cell line and one concentration of small EVs, which could not be confirmed to be equivalent to that in tumor microenvironment, to validate the effect of these small EVs. This means that these effects should be further validated using small EVs from canine DLBCL patients or other DLBCL cell lines in various concentrations. As a further validation, not only the concentration but also the number of small EVs should be measured to determine the amount of EVs. Finally, we could not find any significant changes in secretions of IL-6 and TNFα proteins, whose expressions were increased in mRNA levels by small EV-treatments. It should be one of the causes of these results that we conducted cytokine array analysis at a single point in time after small EV-treatments, and various time points should be set to elucidate the time-dependent change of each cytokine.

In conclusion, canine DLBCL cell line-derived small EVs activate canine peripheral monocytes, possibly through the activation of the TLR and NF-κβ signaling pathways. These activations might result in an increase in the secretion of MCP-1, a cytokine that induces immune cell infiltration of the TME.

CONFLICT OF INTEREST DECLARATION. All of the authors declare that there is no conflict of interest.

ACKNOWLEDGMENTS. This study was supported by the Japan Society for the Promotion of Science, KAKENHI [grant number 17H05043 and 17H03921]. Hirotaka T. received 17H05043 and Hajime T. received 17H03921. The funders had no role in study design, data collection and analysis, decision to publish, or preparation of the manuscript.

REFERENCES

1. Asada, H., Tomiyasu, H., Uchikai, T., Ishihara, G., Goto-Koshino, Y., Ohno, K. and Tsujimoto, H. 2019. Comprehensive analysis of miRNA and protein profiles within exosomes derived from canine lymphoid tumour cell lines. *PLoS One* **14**: e0208567. [Medline] [CrossRef]
2. Atay, S., Gercel-Taylor, C., Suttles, J., Mor, G. and Taylor, D. D. 2011. Trophoblast-derived exosomes mediate monocyte recruitment and differentiation. *Am. J. Reprod. Immunol.* **65**: 65–77. [Medline] [CrossRef]
3. Baj-Krzyworzeka, M., Szatanek, R., Węglarczyk, K., Baran, J., Urbanowicz, B., Brański, P., Ratajczak, M. Z. and Zembala, M. 2006. Tumour-derived microvesicles carry several surface determinants and mRNA of tumour cells and transfer some of these determinants to monocytes. *Cancer Immunol. Immunother.* **55**: 808–818. [Medline] [CrossRef]
4. Bretz, N. P., Ridinger, J., Rupp, A. K., Rimbach, K., Keller, S., Rupp, C., Marmé, F., Umansky, L., Umansky, V., Eigenbrod, T., Sammar, M. and Altevogt, P. 2013. Body fluid exosomes promote secretion of inflammatory cytokines in monocytic cells via Toll-like receptor signaling. *J. Biol. Chem.* **288**: 36691–36702. [Medline] [CrossRef]
5. Bueno, R., Mello, M. N., Menezes, C. A. S., Dutra, W. O. and Santos, R. L. 2005. Phenotypic, functional, and quantitative characterization of canine peripheral blood monocyte-derived macrophages. *Mem. Inst. Oswaldo Cruz* **100**: 521–524. [Medline] [CrossRef]
6. Carvalho, C. M., Bonnefont-Rebeix, C., Picandet, S., Bernaud, J., Phothirath, P., Chabanne, L., Marchal, T., Magnol, J. P. and Rigal, D. 2004. Evaluation of elutriation and magnetic microbead purification of canine monocytes. *Vet. Immunol. Immunopathol.* **101**: 171–178. [Medline] [CrossRef]
7. Cen, X., Liu, S. and Cheng, K. 2018. The Role of Toll-Like Receptor in Inflammation and Tumor Immunity. *Front. Pharmacol.* **9**: 878. [Medline] [CrossRef]
8. Chow, A., Zhou, W., Liu, L., Fong, M. Y., Champer, J., Van Haute, D., Chin, A. R., Ren, X., Gugiu, B. G., Meng, Z., Huang, W., Ngo, V., Kortylewski, M. and Wang, S. E. 2014. Macrophage immunomodulation by breast cancer-derived exosomes requires Toll-like receptor 2-mediated activation of NF-κB. *Sci. Rep.* **4**: 5750. [Medline] [CrossRef]
9. Colombo, M., Raposo, G. and Théry, C. 2014. Biogenesis, secretion, and intercellular interactions of exosomes and other extracellular vesicles. *Annu. Rev. Cell Dev. Biol.* **30**: 255–289. [Medline] [CrossRef]
10. Deshmane, S. L., Kremlev, S., Amini, S. and Sawaya, B. E. 2009. Monocyte chemoattractant protein-1 (MCP-1): an overview. *J. Interferon Cytokine Res.* **29**: 313–326. [Medline] [CrossRef]
11. Hao, Q., Vadgama, J. V. and Wang, P. 2020. CCL2/CCR2 signaling in cancer pathogenesis. *Cell Commun. Signal.* **18**: 82. [Medline] [CrossRef]
12. Herrmann, I., Gotovina, J., Fazekas-Singer, J., Fischer, M. B., Hufnagl, K., Bianchini, R. and Jensen-Jarolim, E. 2018. Canine macrophages can like human macrophages be in vitro activated toward the M2a subtype relevant in allergy. *Dev. Comp. Immunol.* **82**: 118–127. [Medline] [CrossRef]
13. Hinshaw, D. C. and Shevde, L. A. 2019. The tumor microenvironment innately modulates cancer progression. *Cancer Res.* **79**: 4557–4566. [Medline] [CrossRef]
14. Karin, M. and Greten, F. R. 2005. NF-kappaB: linking inflammation and immunity to cancer development and progression. *Nat. Rev. Immunol.* **5**: 749–759. [Medline] [CrossRef]
15. Lee, K. M., An, J. H., Yang, S. J., Park, S. M., Lee, J. H., Chae, H. K., Song, W. J. and Youn, H. Y. 2021. Influence of canine macrophage-derived extracellular vesicles on apoptosis in canine melanoma and osteosarcoma cell lines. *Anticancer Res.* **41**: 719–730. [Medline] [CrossRef]
16. Li, Y. L., Shi, Z. H., Wang, X., Gu, K. S. and Zhai, Z. M. 2019. Tumor-associated macrophages predict prognosis in diffuse large B-cell lymphoma and correlation with peripheral absolute monocyte count. *BMC Cancer* **19**: 1049. [Medline] [CrossRef]
17. Ling, H., Yang, Z., Sun, Y., He, Y., Ju, S., Li, J. and Fu, J. 2020. The impact of diffuse large B-cell lymphoma-derived exosomes on macrophage polarisation and cytokine release. *Arch. Med. Sci.* doi:10.5114/aoms.2020.97355. [CrossRef]
18. Nakatsumi, H., Matsumoto, M. and Nakayama, K. I. 2017. Noncanonical pathway for regulation of CCL2 expression by an mTORC1-FOXK1 axis promotes recruitment of tumor-associated macrophages. *Cell Rep.* **21**: 2471–2486. [Medline] [CrossRef]
19. Opinto, G., Vegliante, M. C., Negri, A., Skrypets, T., Loseto, G., Pileri, S. A., Guarini, A. and Ciavarella, S. 2020. The tumor microenvironment of DLBCL in the computational era. *Front. Oncol.* **10**: 351. [Medline] [CrossRef]
20. Robinson, M. D. and Oshlack, A. 2010. A scaling normalization method for differential expression analysis of RNA-seq data. *Genome Biol.* **11**: R25. [Medline] [CrossRef]
21. Robinson, M. D., McCarthy, D. J. and Smyth, G. K. 2010. edgeR: a Bioconductor package for differential expression analysis of digital gene expression data. *Bioinformatics* **26**: 139–140. [Medline] [CrossRef]
22. Rütgen, B. C., Hammer, S. E., Gerner, W., Christian, M., de Arespacochaga, A. G., Willmann, M., Kleiter, M., Schwendenwein, I. and Saalmüller, A. 2010. Establishment and characterization of a novel canine B-cell line derived from a spontaneously occurring diffuse large cell lymphoma. *Leuk. Res.* **34**: 932–938. [Medline] [CrossRef]
23. Sabroe, I., Parker, L. C., Dower, S. K. and Whyte, M. K. B. 2008. The role of TLR activation in inflammation. *J. Pathol.* **214**: 126–135. [Medline] [CrossRef]
24. Scott, D. W. and Gascoyne, R. D. 2014. The tumour microenvironment in B cell lymphomas. *Nat. Rev. Cancer* **14**: 517–534. [Medline] [CrossRef]
25. Soares Martins, T., Catita, J., Martins Rosa, I., A B da Cruz E Silva, O. and Henriques, A. G. 2018. Exosome isolation from distinct biofluids using precipitation and column-based approaches. *PLoS One* **13**: e0198820. [Medline] [CrossRef]
26. Théry, C., Witwer, K. W., Aikawa, E., Alcaraz, M. J., Anderson, J. D., Andriantsitohaina, R., Antoniou, A., Arab, T., Archer, F., Atkin-Smith, G. K., Ayre, D. C., Bach, J. M., Bachurski, D., Baharvand, H., Balaj, L., Baldacchino, S., Bauer, N. N., Baxter, A. A., Bebawy, M., Beckham, C., Bedina Zavec, A., Benmoussa, A., Berardi, A. C., Bergese, P., Bielska, E., Blenkiron, C., Bobis-Wozowicz, S., Boilard, E., Boireau, W., Bongiovanni, A., Borràs, F. E., Bosch, S., Boulanger, C. M., Breakefield, X., Breglio, A. M., Brennan, M. Á., Brigstock, D. R., Brisson, A., Broekman, M. L. D., Bromberg, J. F., Bryl-Górecka, P., Buch, S., Buck, A. H., Burger, D., Busatto, S., Buschmann, D., Bussolati, B., Buzás, E. I., Byrd, J. B., Camussi, G., Carter, D. R. F., Caruso, S., Chamley, L. W., Chang, Y. T., Chen, C., Chen, S., Cheng, L., Chin, A. R., Clayton, A., Clerici, S. P., Cocks, A., *et al.* 2018. Minimal information for studies of extracellular vesicles 2018 (MISEV2018): a position statement of the International Society for Extracellular Vesicles and update of the MISEV2014 guidelines. *J. Extracell. Vesicles* **7**: 1535750. [Medline] [CrossRef]
27. Tsan, M. F. and Gao, B. 2004. Endogenous ligands of Toll-like receptors. *J. Leukoc. Biol.* **76**: 514–519. [Medline] [CrossRef]
28. Wang, M., Zhao, J., Zhang, L., Wei, F., Lian, Y., Wu, Y., Gong, Z., Zhang, S., Zhou, J., Cao, K., Li, X., Xiong, W., Li, G., Zeng, Z. and Guo, C. 2017. Role of tumor microenvironment in tumorigenesis. *J. Cancer* **8**: 761–773. [Medline] [CrossRef]
29. Whiteside, T. L. 2008. The tumor microenvironment and its role in promoting tumor growth. *Oncogene* **27**: 5904–5912. [Medline] [CrossRef]
30. Zhang, H. G. and Grizzle, W. E. 2014. Exosomes: a novel pathway of local and distant intercellular communication that facilitates the growth and metastasis of neoplastic lesions. *Am. J. Pathol.* **184**: 28–41. [Medline] [CrossRef]
31. Zhu, M. Y., Liu, W. J., Wang, H., Wang, W. D., Liu, N. W. and Lu, Y. 2019. NSE from diffuse large B-cell lymphoma cells regulates macrophage polarization. *Cancer Manag. Res.* **11**: 4577–4595. [Medline] [CrossRef]